Respiratory rate extraction from pulse oximeter and electrocardiographic recordings

IOP PUBLISHING PHYSIOLOGICAL MEASUREMENT

Physiol. Meas. **32** (2011) 1763–1773 doi:10.1088/0967-3334/32/11/S04

Respiratory rate extraction from pulse oximeter and electrocardiographic recordings

Jinseok Lee[1], John P Florian[2] and Ki H Chon[1]

[1] Department of Biomedical Engineering, Worcester Polytechnic Institute, Worcester, MA, USA
[2] Biomedical Research and Development, Navy Experimental Diving Unit, Panama City, FL, USA

E-mail: jinseok@wpi.edu

Received 29 April 2011, accepted for publication 11 July 2011
Published 25 October 2011
Online at stacks.iop.org/PM/32/1763

Abstract

We present an algorithm of respiratory rate extraction using particle filter (PF), which is applicable to both photoplethysmogram (PPG) and electrocardiogram (ECG) signals. For the respiratory rate estimation, 1 min data are analyzed with combination of a PF method and an autoregressive model where among the resultant coefficients, the corresponding pole angle with the highest magnitude is searched since this reflects the closest approximation of the true breathing rate. The PPG data were collected from 15 subjects with the metronome breathing rate ranging from 24 to 36 breaths per minute in the supine and upright positions. The ECG data were collected from 11 subjects with spontaneous breathing ranging from 36 to 60 breaths per minute during treadmill exercises. Our method was able to accurately extract respiratory rates for both metronome and spontaneous breathing even during strenuous exercises. More importantly, despite slow increases in breathing rates concomitant with greater exercise vigor with time, our method was able to accurately track these progressive increases in respiratory rates. We quantified the accuracy of our method by using the mean, standard deviation and interquartile range of the error rates which all reflected high accuracy in estimating the true breathing rates. We are not aware of any other algorithms that are able to provide accurate respiratory rates directly from either ECG signals or PPG signals with spontaneous breathing during strenuous exercises. Our method is near real-time realizable because the computational time on 1 min data segment takes only 10 ms on a 2.66 GHz Intel Core2 microprocessor; the data are subsequently shifted every 10 s to obtain near-continuous breathing rates. This is an attractive feature

since most other techniques require offline data analyses to estimate breathing rates.

Keywords: photoplethysmography, electrocardiography, respiratory rate during exercise, particle filter, metronome breathing, spontaneous breathing

(Some figures in this article are in colour only in the electronic version)

1. Introduction

Monitoring of respiratory rate is of great importance in early detection and diagnosis of potentially dangerous conditions such as sleep apnea (Younes 2008), sudden infant death syndrome (Rantonen *et al* 1998) and chronic obstructive pulmonary disease (Hasselgren *et al* 2001). Respiratory rate is usually measured by using transthoracic impedance plethysmography (Allison *et al* 1964, Ashutosh *et al* 1974, Hamilton *et al* 1967), nasal thermocouples (Marks *et al* 1995) or capnography (Mason *et al* 2000), which measures CO_2 production. However, most of these methods are all labor intensive and expensive by requiring a mask, nasal cannula or wearing chest band sensors. In addition, these devices are uncomfortable, may interfere with natural breathing or sleep positions and are unmanageable in certain applications such as ambulatory monitoring and stress testing.

Recently, the use of photoplethysmography and/or electrocardiogram for respiratory extraction has gained significant interest due to its simplicity and non-invasive measurement capability. The photoplethysmogram (PPG) waveforms and electrocardiogram (ECG) waveforms have been used by several accurate nonparametric methods such as time–frequency spectral analysis (Chon *et al* 2009, Leonard *et al* 2003) and parametric methods such as autoregressive (AR) model-based approaches (Lee and Chon 2010b). Specifically, the continuous wavelet transform (CWT) (Addison and Watson 2004) and variable frequency complex demodulation (VFCDM) (Chon *et al* 2009) methods were utilized to extract either frequency modulation or amplitude modulation seen in the frequency range associated with the heart rate. Both CWT and VFCDM methods have been shown to provide accurate respiratory rate extraction in the low and moderate breathing rates (12–36 breaths per minute). However, the extraction capability of these time–frequency methods became less reliable with increased respiratory rates (Chon *et al* 2009). As a parametric method, an AR model has been adopted by selecting the pole angle with the highest magnitude obtained from resultant coefficients. The AR model was aided by the optimal parameter search (OPS) criteria (Wang *et al* 2002, Zhao *et al* 2004), and the resultant parameters were factorized into multiple pole terms. The method showed more accurate respiratory rate extraction especially for high breathing rates (36–48 breaths min^{-1}) (Lee and Chon 2010b). However, as the signal-to-noise ratio (SNR) decreases, the probability increases that incorrect poles are associated with the highest magnitude, which ultimately affects the accuracy of the method.

Recently, we have developed time-varying approaches to better estimate respiratory rates (Lee and Chon 2010a, 2011) by accounting for nonstationary dynamics in pulse oximeter devices as the latter modality can also be used to estimate breathing rates. Using a variant of the particle filtering approach on metronome breathing experimental data, we have demonstrated that accurate breathing rates in the range of 12–90 breaths min^{-1} can be obtained (Lee and Chon 2010a). In the former study, metronome-controlled breathing rates were used to verify the algorithm, but the main disadvantage is that the controlled breathing artificially reduces nonstationary respiratory dynamics during data collection. In addition, while subjects were

breathing spontaneously during exercise, the duration could not be sustained for more than 2 min, and a metronome-controlled respiratory protocol does not truly simulate exercise-induced high breathing rates.

Thus, the goal of this study was to examine the robustness of our particle filter (PF) approach to extract respiratory rates directly from ECG signals as well as PPG signals. Also, the robustness was examined for spontaneous breathing during exercise as well as for metronome breathing. While there have been some studies to extract breath-by-breath respiratory rates directly from an ECG and a pulse oximeter (Dash *et al* 2010, Yoshida *et al* 2007), our study is one of the few that examine this capability on both metronome and spontaneous breathing, a feat which has not been successful to date.

2. Materials and methods

2.1. Subjects

Fifteen healthy subjects for metronome breathing and 11 healthy subjects for spontaneous breathing during exercise participated in the study. For the metronome breathing, 7 females and 8 males of age 21.0 ± 1.2 years were involved. None of the subjects had cardiorespiratory or related pathologies. For the spontaneous breathing, 11 males of age 36.0 ± 1.0 years were involved, and each subject underwent a complete medical screening, including complete blood count, complete metabolic panel, lipid profile evaluation, urinalysis, physical examination, skinfold body fat measurement and determination of maximal oxygen uptake ($\dot{V}O_{2\,\mathrm{max}}$). All subjects were healthy, active and normotensive nonsmokers who were not taking any medications that would affect responses in the study. Approval was obtained from the Institutional Review Board of the Navy Experimental Diving Unit. Each subject gave written informed consent, and all procedures conformed to the Declaration of Helsinki.

2.2. Experimental set-up and measurements

The metronome and spontaneous breathing experiments were performed by collecting PPG and ECG waveforms, respectively. In the metronome breathing experiment, we used an MP506 pulse oximeter (Nellcor Oximax, Boulder, CO) reusable sensor (Durasensor DS-100A), which incorporates a conditioning circuit and has an analog output of 4.864 kHz. The PPG waveforms were collected on 15 healthy subjects with metronome respiratory rates ranging from 0.4 to 0.6 Hz at an increment of 0.1 Hz. The PPG data were collected in the supine and upright positions for subjects instructed to breathe at each breathing rate (i.e. 0.4, 0.5 and 0.6 Hz). The pulse oximeter sensor was attached to the subjects' left index or middle finger. The subjects were instructed to breathe at a constant rate according to a timed beeping sound so that the subjects inhaled and exhaled when the beeping sound was heard. Three minutes of PPG data were collected for each position for each breathing rate. We also simultaneously measured respiration signals using the Respitrace system, which uses inductive plethysmography to provide calibrated voltage outputs corresponding to rib cage and abdominal compartment volume changes. From the Respitrace system, true respiratory rates were evaluated by counting the number of peaks in a given minute.

In the spontaneous breathing experiment, ECG signals were recorded by a five-lead surface ECG (Dash 3000, General Electric). Respiratory frequency (turbine flowmeter) and $\dot{V}O_2$ were measured using a breath-by-breath gas exchange analyzer (COSMED K4b^2), which was calibrated before each test according to the manufacturer's instructions. The flowmeter and gas sampling line connect to a sealed oro-nasal face mask. Data from the COSMED K4b^2

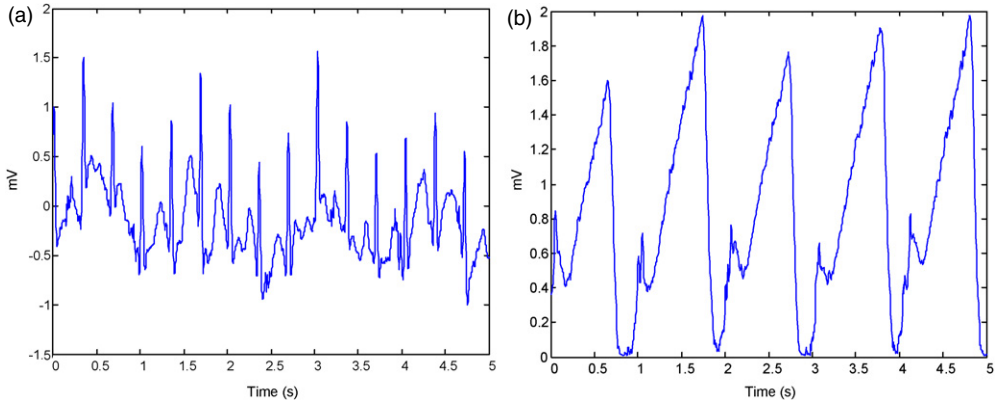

Figure 1. Representative recordings of the ECG (left panel) and pulse oximeter (right panel) data.

were acquired using associated COSMED software. ECG data were sampled and logged at 400 Hz in LabVIEW (National Instruments). Eleven subjects completed a submaximal exercise trial after a single 6 h oxygen dive. After abstaining from alcohol for 2 days and caffeine for 1 day before the exercise trial, and dressed in running shorts and a t-shirt, each subject reported to the laboratory between 8 am and 10 am. The subjects were instrumented with ECG leads for measurement of *R–R* interval, and with a mask to determine respiratory frequency and for expired gas analysis. For each exercise trial, the subjects ran on a treadmill (Pro XL, Woodway) at a workload corresponding to 85% of their respective $\dot{V}O_{2\ \max}$ (Franklin *et al* 2000) until volitional fatigue. Each subject was encouraged to give the maximum effort. Respiration for each subject during exercise trials was not controlled. The chosen workload provided a sufficient stimulus to continuously increase respiratory frequency over the duration of the exercise trial. The left and right panels of figure 1 show representative recordings of the ECG and pulse oximeter data, respectively.

2.3. AR model for respiratory rate candidates

Respiratory rate starts from an AR model:

$$x(n) = -\sum_{k=1}^{K} a_k x(n-k) + e(n), \tag{1}$$

where K is the model order, a_k are the unknown coefficients and $e(n)$ is the prediction error. By using OPS criteria, we obtain accurate parameter estimation among the over-determined model order K. The OPS can be designed to automatically select the optimal model order for any signal and, thus, can be tuned to each signal without any human subjectivity. With any initial model order of K, the significant model order K_{opt} is determined by the ratio of two neighboring projection distances (Zou *et al* 2003). Once the unknown AR parameters, a_k, are estimated, they are formulated as the transfer function $H(z)$ as shown below:

$$H(z) = \frac{1}{\sum_{k=1}^{K_{\text{ops}}} a_k z^{-k}} = \frac{z^{K_{\text{ops}}}}{(z-z_1)(z-z_2)\cdots(z-z_{K_{\text{ops}}})}, \tag{2}$$

where the AR coefficients are factorized into K_{ops} pole terms, where $K_{\text{ops}} \leqslant K$. The real and complex conjugate poles define the power spectral peaks with the larger magnitude poles corresponding to the greater magnitudes (Lee and Chon 2010b). The resonant frequency of

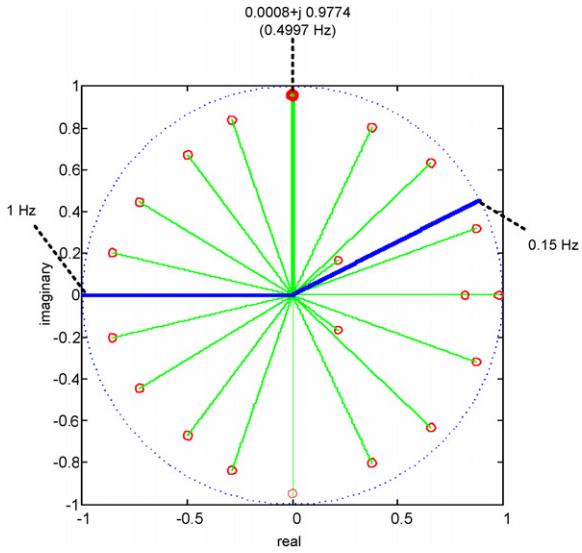

Figure 2. Graphical representation of poles.

each spectral peak is given by the phase angle of the corresponding pole; the phase angle θ of a pole at frequency f is defined as $2\pi f \Delta t$, where Δt is the sampling interval. Among the poles, we set the region of interest for respiratory rates between f_{low} and f_{high} (e.g. 0.15 and 1.0 Hz). Let us denote the number of pole angles within the region of interest by K_{roi}. If $K_{\text{roi}} \geqslant 2$, the pole with the highest magnitude is chosen to be representative of the respiratory rate. In previous studies, the OPS showed better performance than both CWT- (Leonard *et al* 2003, Clifton *et al* 2007, Addison and Watson 2004) and VFCDM-based (Chon *et al* 2009, Wang *et al* 2006) time–frequency spectral techniques. The AR model approach to the respiratory rate extraction approach requires prefiltering of the PPG waveforms in order to minimize the cardiac effects. Thus, the ECG or PPG waveforms are detrended, filtered and downsampled to 2 Hz so that we can increase the angular resolution between 0 and 1 Hz.

To illustrate the phase angle of poles for respiratory rate extraction, we tested a 60 s segment PPG signal with respiratory rate of 0.5 Hz, heart rate of 1.1 Hz and sampling rate of 200 Hz. The resultant poles are shown in figure 2. We set f_{low} and f_{high} as 0.15 and 1.0 Hz, respectively, and found the pole (0.0008 + j0.9774) with the highest magnitude; the corresponding angle results in the respiratory rate of 0.4997 Hz which is close to the true respiratory rate of 0.5 Hz. However, the pole angle with the highest magnitude may not always lead to accurate estimation of the respiration due to low SNR or interaction among poles. To improve the accuracy of an AR model approach, we combine it with the PF algorithm.

2.4. PF for final respiratory rate estimation

Given a true waveform of either a PPG or an ECG signal from time $n - n_{\text{seg}}$ to time n denoted by $S_{n-n_{\text{seg}}:n}$, we define the respiratory rate at time n as $R(n)$, where n_{seg} is the signal segment length. By using the OPS technique and the breathing rates' region of interest, we obtain the measurement vector $\boldsymbol{P}(n)$ including K_{roi} pairs of pole angles and their magnitudes:

$$\boldsymbol{P}(n) = \left[p_1^a \; p_2^a \cdots p_k^a \cdots p_{K_{\text{roi}}}^a \; p_1^m \; p_2^m \cdots p_k^m \cdots p_{K_{\text{roi}}}^m\right]^T, \tag{3}$$

where p_k^a and p_k^m represent the kth pole angle and magnitude, respectively. Under the assumption that the respiratory state is a Markov process, the respiratory state can be modeled as

$$R(n) = T(R(n - n_{\text{sam}}), Q(n)) = R(n - n_{\text{sam}}) + Q(n), \tag{4}$$

where n_{sam} is the time interval at which the respiration is considered, $T(\cdot)$ is a known, not necessarily linear function of the previous state at the time sample $n - n_{\text{sam}}$ and $Q(n)$ is a noise term which is not necessarily Gaussian. We assume that $R(n)$ is a stationary process.

Let $P(n_0 : n) = [P(n_0) \cdots P(n - n_{\text{sam}})P(n)]$ denote the concatenation of all measurements up to time n, where n_0 is the initial time. The aim is to recursively estimate the conditional probability density $p(R(n)|P(1 : n))$ from which the respiratory rate can be obtained as the mean of the density function. In practice, the posterior probability density is not available. However, assuming that the posterior probability density at time $n - n_{\text{sam}}$ is available, the posterior probability density at time n can be found through the Chapman–Kolmogorov equation and Bayes' rule:

$$p(R(n)|\boldsymbol{P}(n_0 : n - n_{\text{sam}})) = \int p(R(n)|R(n_0 - n_{\text{sam}})) \cdot p(R(n_0 - n_{\text{sam}})|\boldsymbol{P}(n_0 : n - n_{\text{sam}})) \cdot \mathrm{d}R(n_0 - n_{\text{sam}}), \tag{5}$$

$$p(R(n)|\boldsymbol{P}(n_0 : n)) \propto p(\boldsymbol{P}(n)|R(n)) \cdot p(R(n)|\boldsymbol{P}(n_0 : n - n_{\text{sam}})), \tag{6}$$

where $p(R(n)|\boldsymbol{P}(n_0 : n - n_{\text{sam}}))$ is the posterior probability density, $p(R(n)|R(n - n_{\text{sam}}))$ is the state transition density, $p(R(n)|\boldsymbol{P}(n_0 : n))$ is the prediction probability density and $p(\boldsymbol{P}(n)|R(n))$ is the likelihood. For the solution of equations (5) and (6), we used a PF approach, which is suitable for non-Gaussian problems, and approximated equations (5) and (6) via Monte Carlo simulations by representing the density function with a set of particles.

In the PF algorithm, a set of particles is generated, and the particles represent a prior probability density function $p(R(n)|\boldsymbol{P}(n_0 : n - n_{\text{sam}}))$. Given the particles corresponding to the posterior probability density function of $p(R(n - n_{\text{sam}})|\boldsymbol{P}(n_0 : n - n_{\text{sam}}))$ obtained at time $n - n_{\text{sam}}$, new particles are generated at time n. After the new particles corresponding to the prior probability density function $p(R(n)|\boldsymbol{P}(n_0 : n - n_{\text{sam}}))$ are generated, each particle weight should be evaluated based on the measurement vector $\boldsymbol{P}(n)$ which is obtained via OPS criteria. The weighted particles represent the posterior probability density function of $p(R(n)|\boldsymbol{P}(n_0 : n))$. For the particle weight evaluation, we use the strongest neighbor (SN) likelihood, in which the measurement with the highest intensity among the validated measurements is used and the others are discarded (Bar-Shalom 1990). The SN likelihood is evaluated as

$$w^i(n) = \exp\left(-\frac{\left(R^1(n) - p_{\max}^a\right)^2}{2\sigma_{\text{gau}}^2}\right), \tag{7}$$

where $i = 1, 2, \ldots, N$ for the number of particles, and $p_{\max}^a$ is the pole angle with the highest pole magnitude among the pole angles.

Subsequently, we normalize the particle weight and calculate the mean of the particles' posterior probability density for the respiratory rate. In addition, we resample the particles to generate new particles at the next time instant, $n + n_{\text{sam}}$, to reduce the effect of the degeneracy problem. However, it can lead to a loss of diversity of the particles. For example, the resultant resampled particles may contain many repeated points due to the resampling algorithm, which may lead to all particles collapsing to a single point in the worst case scenario. Consequently, a set of resampled particles may incorrectly represent the posterior probability density and can also lead to the incorrect prior probability density function. We can overcome this limitation

by using a particle diversity loss measure, the effective sample size N_{eff} (Arulampalam *et al* 2002) defined by

$$N_{\text{eff}}(n) = \frac{I}{1 + \text{Var}(\bar{w}^{*i}(n))} \approx \frac{1}{\sum_{i=1}^{I} (\bar{w}^{i}(n))^2}, \tag{8}$$

where $\bar{w}^{*i}(n)$ and $\bar{w}^{i}(n)$ are the ith true particle weight and ith normalized particle weight, respectively. Hence, when $\frac{1}{\sum_{i=1}^{I} (\bar{w}^{i}(n))^2}$ is smaller than $I/2$ (Yu *et al* 2010), we replace the resultant posterior density function by a previously obtained posterior density function defined as $p(R(n)|\boldsymbol{P}(n_0 : n)) = p(R(n - n_{\text{sam}})|\boldsymbol{P}(n_0 : n - n_{\text{sam}}))$. Since respiratory rate changes slowly in most cases, the replacement approach does not affect the overall performance.

2.5. Data analysis

We performed the respiratory rate estimation on 60 s segments. All data segments were shifted by 10 s for the entire PPG and ECG recording. We set the initial model order K to 30 for the OPS. The respiratory rate of interest was set to $f_{\text{low}} = 0.15$ Hz and $f_{\text{high}} = 1.0$ Hz. The PF parameters were set to $\sigma^2_{\text{gen}} = 0.02$, $\sigma^2_{\text{gau}} = 0.004$ and $I = 100$, where σ^2_{gen} represents the generated particle variance, σ^2_{gau} is the likelihood variance and I is the number of particles (Lee and Chon 2010a). For an initial set of particles, the pole angle with the highest magnitude at the beginning of the time sample was chosen. Since PF provides different results at each realization due to randomly generated particles, we tested 100 realizations. Each calculated respiratory rate time corresponds to the end of each segment. For each 60 s ($n_{\text{seg}} = 60$) ECG or PPG segment, the 100 realizations of the combined PF and AR model were performed and averaged to provide a single breathing rate estimate. In order to compare the performance of the two methods consisting solely of the AR and of the AR model with the PF method, we first calculated the percentage error with every 60 s data segment with 10 s interval ($n_{\text{sam}} = 10$) for each method as

$$\text{Error rate}(\%) = \left| \frac{\text{True respiratory rate} - \text{Estimated respiratory rate}}{\text{True respiratory rate}} \right| \times 100. \tag{9}$$

Especially for the spontaneous breathing data, the true respiratory rate was obtained as the average rate over each 60 s segment obtained from the reference breath gas exchange analyzer. The error rates were calculated from all subjects. We next quantified the accuracy by using the mean, standard deviation and interquartile range (IQR) of the error rates. The paired t-test was performed to test the significance of the AR method and the AR model with the PF method. A p-value < 0.01 was considered significant.

3. Results

Figure 3 shows a single realization of respiratory rate estimation by an AR model with and without PF for different metronome breathing rates of 0.4, 0.5 and 0.6 Hz. Three minutes of data from one subject in the upright position are shown. In all cases, the AR model with PF resulted in more accurate estimation than the AR model without PF for the entire PPG recordings. More specifically, based on the AR model only, some incorrect poles are associated with the highest magnitude due to motion and noise artifact, and thus some incorrect breathing rates are chosen. However, the PF overcomes this limitation and allows estimation of breathing rates that are closer to the true rates.

Table 1 summarizes the entire spontaneous breathing data analysis with mean, standard deviation and IQR of the estimated error rates from 15 subjects in both supine and upright

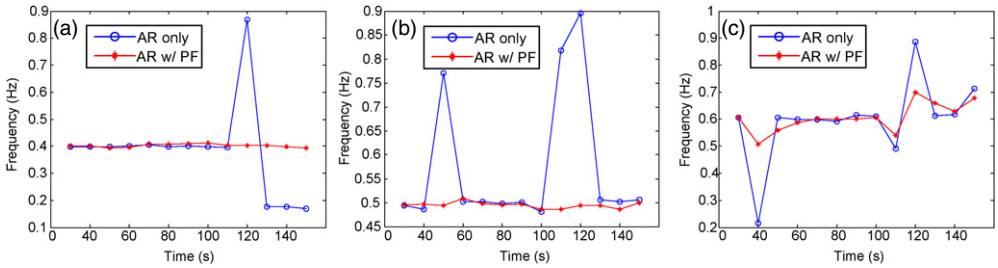

Figure 3. A single realization of respiratory rate estimation from PPG recording with metronome breathing: (a) true rate of 0.4 Hz (heart rate of 1.0 Hz), (b) true rate of 0.5 Hz (heart rate of 1.1 Hz) and (c) true rate of 0.6 Hz (heart rate of 1.3 Hz). Three minutes of data from one subject in the upright position are shown.

Table 1. Comparison of the AR model with and without PF in both supine and upright positions. Mean, standard deviation and IQR are shown with metronome breathing rates ranging from 0.4 to 0.6 Hz.

Position	Supine		Upright	
Methods	AR only	AR w/PF	AR only	AR w/PF
Mean ± std of ER (Hz)	17.37 ± 20.10	6.00 ± 6.34	11.21 ± 20.61	3.47 ± 3.62
IQR of ER (Hz)	28.75	6.65	10.72	3.53
Heart rate (Hz)	0.9–1.6		0.9–1.8	

Table 2. Comparison of the AR model and the AR model with PF in different frequency ranges. Mean, standard deviation and IQR are shown with spontaneous breathing rates.

Frequency range (Hz)	0.6–0.8 Hz		0.8–1.0 Hz	
Methods	AR only	AR w/PF	AR only	AR w/PF
Mean ± std of ER (Hz)	19.09 ± 24.12	3.87 ± 3.54	29.27 ± 22.09	7.22 ± 8.00
IQR of ER (Hz)	28.40	3.85	42.23	5.36
Heart rate (Hz)	1.8–2.8		2.4–3.4	

positions. For the mean, standard deviation and IQR of the error rates, the AR model with PF was significantly smaller than the AR model without PF for all data sets regardless of the body postures. In the supine position, the mean, standard deviation and IQR of the AR model with PF were 2.90, 3.17 and 4.32 times smaller than those of the AR model without PF, respectively. Similarly, in the upright position, the mean, standard deviation and IQR of the AR model with PF were 3.23, 5.69 and 3.04 times smaller than those of the AR model without PF, respectively. All of the results between the two methods are statistically significant with $p < 0.01$.

Figure 4 shows a single realization of respiratory rate estimation by the AR model with and without PF for spontaneous breathing during exercise. Similar to the metronome breathing data, based on the AR model only, some incorrect poles are associated with the highest magnitude due to motion and noise artifact, and thus many of the chosen breathing rates are incorrect. By incorporating the PF, the estimated breathing rates are able to track the true respiratory patterns throughout the entire ECG recording.

Table 2 summarizes the entire spontaneous breathing data analysis with mean, standard deviation and IQR of the estimated error rates from 11 subjects in different frequency ranges:

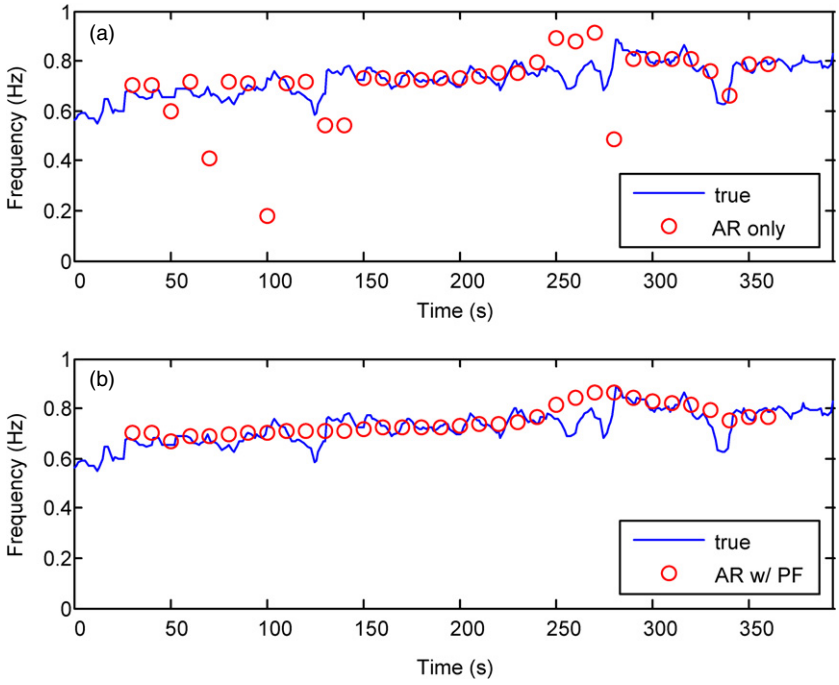

Figure 4. A single realization of respiratory rate estimation from ECG recording with spontaneous breathing (heart rate of 1.9 Hz): (a) AR model without PF-based breathing rate estimation and (b) AR model with PF-based breathing rate estimation.

0.6 to 0.8 Hz and 0.8 to 1.0 Hz. For the mean, standard deviation and IQR of the error rates, the AR model with PF was significantly smaller than the AR model without PF for all data sets regardless of frequency ranges. In the frequency range between 0.6 and 0.8 Hz, the mean, standard deviation and IQR of the AR model with PF were 4.93, 6.81 and 7.38 times smaller than those of the AR model without PF, respectively. Similarly, in the frequency range between 0.8 and 1.0 Hz, the mean, standard deviation and IQR of the AR model with PF were 4.05, 2.77 and 7.88 times smaller than those of the AR model without PF, respectively. All of the results between the two methods are statistically significant with $p < 0.01$.

For all experimental conditions, the AR model with PF resulted in better accuracy in the respiratory rate estimation than the AR model without PF. We also determined the computational time of the AR model with PF to determine if the real-time realization of the algorithm is possible. It was found that the computational time to extract respiratory rates on 1 min data segments averaged only 0.01 s (Matlab R2009b). Thus, real-time update of respiratory rates is certainly feasible.

4. Discussion

We demonstrated a robust time-varying and nonlinear PF approach to accurately extract respiratory rates directly from PPG and ECG signals under both conditions of metronome and spontaneous breathing. The PF technique has been widely adopted in many estimation problems, especially for nonlinear and time-varying conditions (Arulampalam *et al* 2002). Estimation of respiratory rate works by the use of a standard AR method followed by

factorization of the estimated AR parameters via the PF into multiple pole terms. The pole with the highest magnitude is chosen to represent a respiratory rate (Lee and Chon 2010a). However, the performances of PF methods are affected by the initial set of particles chosen. In this paper, the initial set of particles was chosen based on the pole angle with the highest magnitude as determined by the OPS. The accuracy of the PF method will certainly benefit and converge faster to a true solution if the initially chosen set of particles is closest to the true respiratory rate. This is the primary reason why we have combined the OPS with PF to obtain near-optimal solutions. For more accurate results than those presented in this work, a method which provides the optimal initial set of particles will need to be investigated. Since the initial setting is one of the PF inherent limitations, a reasonable initial set of particles should be examined. Certainly, one approach that can be used to resolve this problem is to utilize a time-variant AR estimator.

5. Conclusion

We presented an algorithm for the respiratory rate extraction using a particle filter (PF) approach, which is applicable to both photoplethysmogram (PPG) and electrocardiogram (ECG) signals. In addition, we have demonstrated the robustness of the proposed algorithm under both metronome and spontaneous breathing conditions. Our PF method is real-time realizable by the fact that the computational time on 1 min ECG data takes only 10 ms in a 2.66 GHz Intel Core2 microprocessor. This is an attractive feature since current technologies require attaching multiple sensors for obtaining vital signs as well as ECG electrodes, which can all consume several minutes. All that is required for our approach to be commercially viable is to embed the algorithm into a microprocessor of existing ECG devices or pulse oximeters.

References

Addison P S and Watson J N 2004 Secondary transform decoupling of shifted nonstationary signal modulation components: application to photoplethysmograph *Int. J. Wavelets Multiresolut. Inf. Process.* **2** 43–57

Allison R D, Holmes E L and Nyboer J 1964 Volumetric dynamics of respiration as measured by electrical impedance plethysmography *J. Appl. Physiol.* **19** 166–73

Arulampalam M S, Maskell S, Gordon N and Clapp T 2002 A tutorial on particle filters for online nonlinear/non-Gaussian Bayesian tracking *IEEE Trans. Signal Process.* **50** 174–88

Ashutosh K, Gilbert R, Auchincloss J H, Erlebacher J and Peppi D 1974 Impedance pneumograph and magnetometer methods for monitoring tidal volume *J. Appl. Physiol.* **37** 964–6

Bar-Shalom Y 1990 University of California, Los Angeles University Extension *Multitarget-Multisensor Tracking: Applications and Advances* (Boston, MA: Artech House)

Chon K H, Dash S and Ju K 2009 Estimation of respiratory rate from photoplethysmogram data using time–frequency spectral estimation *IEEE Trans. Biomed. Eng.* **56** 2054–63

Clifton D, Douglas J G, Addison P S and Watson J N 2007 Measurement of respiratory rate from the photoplethysmogram in chest clinic patients *J. Clin. Monit. Comput.* **21** 55–61

Dash S, Shelley K H, Silverman D G and Chon K H 2010 Estimation of respiratory rate from ECG, photoplethysmogram, and piezoelectric pulse transducer signals: a comparative study of time–frequency methods *IEEE Trans. Biomed. Eng.* **57** 1099–107

Franklin B A, Whaley M H and Howley E T 2000 *American College of Sports Medicine, ACSM's Guidelines for Exercise Testing and Prescription* (Philadephia, PA: Lippincott Williams and Wilkins)

Hamilton L H, Beard J D, Carmean R E and Kory R C 1967 An electrical impedance ventilometer to quantitate tidal volume and ventilation *Med. Res. Eng.* **6** 11–6

Hasselgren M, Arne M, Lindahl A, Janson S and Lundback B 2001 Estimated prevalences of respiratory symptoms, asthma and chronic obstructive pulmonary disease related to detection rate in primary health care *Scand. J. Prim. Health Care* **19** 54–7

Lee J and Chon K H 2010a An autoregressive model-based particle filtering algorithms for extraction of respiratory rates as high as 90 breaths per minute from pulse oximeter *IEEE Trans. Biomed. Eng.* **57** 2158–67

Lee J and Chon K H 2010b Respiratory rate extraction via an autoregressive model using the optimal parameter search criterion *Ann. Biomed. Eng.* **38** 3218–25

Lee J and Chon K 2011 Time-varying autoregressive model-based multiple modes particle filtering algorithm for respiratory rate extraction from pulse oximeter *IEEE Trans. Biomed. Eng* **58** 7904

Leonard P, Beattie T F, Addison P S and Watson J N 2003 Standard pulse oximeters can be used to monitor respiratory rate *Emerg. Med. J.* **20** 524–5

Marks M K, South M and Carter B G 1995 Measurement of respiratory rate and timing using a nasal thermocouple *J. Clin. Monit. Comput.* **11** 159–64

Mason K P, Burrows P E, Dorsey M M, Zurakowski D and Krauss B 2000 Accuracy of capnography with a 30 foot nasal cannula for monitoring respiratory rate and end-tidal CO_2 in children *J. Clin. Monit. Comput.* **16** 259–62

Rantonen T, Jalonen J, Gronlund J, Antila K, Southall D and Valimaki I 1998 Increased amplitude modulation of continuous respiration precedes sudden infant death syndrome—detection by spectral estimation of respirogram *Early Hum. Dev.* **53** 53–63

Wang H, Lu S, Ju K and Chon K H 2002 A new approach to closed-loop linear system identification via a vector autoregressive model *Ann. Biomed. Eng.* **30** 1204–14

Wang H, Siu K, Ju K and Chon K H 2006 A high resolution approach to estimating time–frequency spectra and their amplitudes *Ann. Biomed. Eng.* **34** 326–38

Yoshida Y, Yokoyama K and Ishii N 2007 Real-time continuous estimation of respiratory frequency during sleep based on heart rate time series *Conf. Proc. IEEE. Eng. Med. Biol. Soc.* **2007** 648–51

Younes M 2008 Role of respiratory control mechanisms in the pathogenesis of obstructive sleep disorders *J. Appl. Physiol.* **105** 1389–405

Yu J-X, Tang Y-L and Liu W-J 2010 Adaptive mutation particle filter based on diversity guidance *Int. Conf. on Machine Learning and Cybernetics (Qingdao)* pp 369–74

Zhao H, Zou R and Chon K H 2004 Estimation of time-varying coherence function using time-varying transfer functions *Conf. Proc. IEEE Eng. Med. Biol. Soc.* **1** 298–301

Zou R, Wang H and Chon K H 2003 A robust time-varying identification algorithm using basis functions *Ann. Biomed. Eng.* **31** 840–53